

Supporting Information

Boosting the methanol selectivity in CO₂ hydrogenation over MOF-derived
CuZn@CN catalyst via Rb incorporation

Jyoti Gahtori^{a, b, 1}, Jyotishman Kaishyop^{a, b, 1}, Gaje Singh^{a, b}, Tuhin S. Khan^{a, b}, Flavio C.
Vicentin^c, Tulio C.R. Rocha^c, Ankur Bordolo^{a, b, *}

^a Light and Stock Processing Division, CSIR-Indian Institute of Petroleum (IIP), Dehradun-
248005, India

^b Academy of Scientific and Innovative Research (AcSIR), Ghaziabad-201002, India

^c Brazilian Synchrotron Light Laboratory (LNLS), Brazilian Center for Research on Energy
and Materials (CNPEM), 13083-100, Brazil

Table of Contents

1	Experimental section	3
1.1	Materials and method	3
1.2	Preparation of the catalyst	3
1.2.1	Synthesis of Cu-ZnO MOF	3
1.2.2	Loading of cobalt and alkali-metal promotors.....	3
1.3	Catalytic activity test	4
1.4	Physicochemical characterization	4
1.5	DFT Method	5
2	Characterizations for spent catalyst.....	6
3	Stability test of the catalyst	7
Figure S1	EDS mapping for fresh 2.5Rb5Co-CuZn catalyst	8
Figure S2	XPS spectra for spent 5Rb5Co-CuZn	9
Figure S3	TEM images for spent 5Rb5Co-CuZn	9
Figure S4	Elemental mapping of spent 5Rb5Co-CuZn	10
Figure S5	Characterization of spent 5Rb5Co-CuZn catalyst (a) XRD (b) N ₂ physisorption isotherm, (inset) pore size distribution (c) TEM images, (inset) particle size distribution (e) HR-TEM (f) SAED.....	11
Table S1	Surface area, surface composition determined from EDS mapping, and total CO ₂ uptake	12
Table S2	AFTS activity and selectivity for different dispersible NPs and supported catalyst	13
Table S3	The representation of deviation in CO ₂ hydrogenation for 5Rb5C-CuZn catalyst	14
3	Reference	15

1. Experimental section

1.1. Material and methods: The chemicals, solvents, and metal precursors utilized in this study were supplied by Sigma Aldrich and were not purified or modified. Sigma Gas Service provided all of the required gases, which were purified to > 99.99% purity.

1.2. Preparation of the catalyst: The required catalysts were synthesized in two steps:

1.2.1. Synthesis of Cu-ZnO MOF: The catalyst was synthesized by a previously reported procedure with a few modifications¹. Here, 21.10 g of 2-MIM (2-methyl imidazole) was added to the stirred suspension of CuO (15.91 g, 0.20 mol) and ZnO (8.14 g, 0.10 mol) in 120 g of 1% aq. acetic acid. The mixture was heated at 363 K for 30 min. The resulting green solids were separated by filtration followed by washing with water and drying at 373 K.

1.2.2. Loading of cobalt and alkali-metal promoters: The synthesized green solids were further loaded with alkali-metal promoters along with 5 wt.% cobalt. Initially, the required amount of Cu-Zn MOF was dispersed in 20 mL of water. Then the measured amount of metal (alkali) nitrate and cobalt nitrate was added to the same solution to achieve 2.5 wt.% and 5 wt.% of alkali metal and cobalt, respectively, in the catalyst. It was followed by the freeze-drying of the catalyst using a lyophilizer, which was kept for the time being to evaporate the water completely. The final catalyst was obtained by carbonizing the dried product at 1173 K for 3 h in the presence of flowing N₂.

The other catalysts were prepared by following a similar procedure, where the amount of metal precursors was varied according to the required compositions in the catalyst. For easy demonstration, the catalysts have 5 wt.% Co and 2.5 wt.% of Na, K, Rb, and Cs will be designated 2.5Na5Co-CuZn, 2.5K5Co-CuZn, 2.5Rb5Co-CuZn, and 2.5Cs5Co-CuZn respectively. Similarly, the numerical value will represent the composition of alkali metal and cobalt in the other used catalysts.

1.3. Catalytic activity test: The aqueous phase CO₂ hydrogenation to methanol was tested in a high-pressure stainless steel 100 mL batch reactor (Parr instrument). The catalyst was dispersed in 40 mL of water before being added to the reactor. To avoid contaminants, the reactor was purged twice with reaction mixture gas (CO₂: H₂: N₂ = 1: 3: 1), then sealed and pressured to 6.0 MPa with reaction gas. At a stirring speed of 700 rpm, the CO₂ hydrogenation productivity was measured at 473 K. Once the reaction temperature was reached, the reaction was carried out for 20 h for each catalyst.

Once the reaction was completed, the reactor was cooled to room temperature, and the gaseous products were examined using an online gas analyzer (Agilent 7890B). A Molsieve 5A column was used to separate gasses H₂, CO₂, N₂, CH₄, and CO, which were subsequently quantified by a thermal conductivity detector (TCD). The aqueous phase composition after the reaction was analyzed by the DB-WAX column attached with FID to identify the distribution of alcoholic products. The amount of methanol was calculated by comparing the area of the product with the calibration curve made by different concentration of methanol in water and the selectivity was calculated by carbon balancing. In each case, the carbon balance was >85%.

1.4. Physicochemical characterization: A Proto Advance X-ray diffractometer with a Cu K radiation source and a Lynx eye high-speed strip detector was used to perform XRD at room temperature. The patterns were collected using a 30 kV X-ray in the range of $2\theta = 5^\circ$ - 80° with a 0.05° step size (dwell time=1s). N₂ adsorption–desorption isotherms were recorded using a Micromeritics ASAP 2020 to investigate the pore architecture in the produced catalyst. The catalyst was degassed in a vacuum at 623 K before each measurement. TEM images were collected using a Jeol JEM 2100 microscope. The samples were prepared by mounting an ethanol-dispersed sample on a lacey carbon Formvar-coated Cu grid. The elemental mapping was also carried out with energy-dispersive X-ray spectroscopy (EDXS) installed in HR-TEM.

The temperature-programmed reduction (TPR) and CO₂ temperature-programmed desorption (TPD) experiments were carried out in Micromeritics, Auto Chem II 2920 instrument attached with a thermal conductivity detector (TCD). Before recording TPR and TPD curve, the surface of the sample was flushed with flowing He at 623 K for 2 h to remove any surface contamination. For measurement of TPR, after flushing with the He, the catalyst was then exposed to a flow of 10% H₂ in He as the temperature was raised to 1173 K (10 K/min). A thermal conductivity detector (TCD) detected the change in the H₂ concentration in the effluent.

To obtain CO₂ TPD, the sample was first reduced at 550 K to ensure the reduction of any auto-oxidised species on the surface. The sample was cooled under flowing hydrogen to 373 K and it was held at 373K under flowing helium to remove physisorbed and/or weakly bound species. The CO₂ was adsorbed at 373 K for 30 min and the sample was held at the same temperature under flowing argon to remove physisorbed and/or weakly bound species, prior to increasing the temperature slowly to 800K. The TPD spectrum was integrated and the number of moles of desorbed CO₂ determined by comparing to the areas of calibration pulses of CO₂ in He.

Using Thermo Scientific K-alpha X-ray photoelectron spectroscopy, the oxidation status of several active metals in the samples was determined (XPS). The binding energy of C 1 s at 284.8 eV was taken as a reference to calibrate the binding energies of each element. The XAS experiment was performed at the XAS/XPS branch of the IPE beamline of the Sirius light source at the Brazilian Synchrotron Light Laboratory.

1.5. DFT Method

All DFT calculations reported in this work have been performed by using Vienna Ab-initio Simulation Package (VASP) version 5.3.5.². The projector-augmented wave (PAW) pseudopotentials³ along with generalized gradient approximation (GGA) Revised Perdew-

Burke-Ernzerhof (RPBE) exchange-correlation functional were utilized⁴. A cut-off energy of 396 eV was used. For structure optimizations, the energy and force convergence criteria have been set to 1×10^{-6} eV and 0.05 eV/Å, respectively. The Monkhorst–Pack k-point sampling of $2 \times 2 \times 1$ was used for slab calculations.

The ZnO (100) surfaces were modelled using a three-layer surface slab. The Cu₁₃ metal nanocluster was grafted over ZnO (100) surfaces to obtain Cu₁₃/ZnO (100) catalyst surface. The Cu₁₃/ZnO (100) surface was further modified with the replacement of one Cu atom with Co, followed by the addition of alkali metals (Na, K, Rb, and Cs) to the surface oxygen of ZnO. For all the DFT geometry optimization calculations the bottom two layers of the surface slabs were kept fixed, whereas the top one layer along with the Co-Cu₁₂ cluster and adsorbates were allowed to relax. For all the surface slabs, a vacuum of 25 Å was employed in the z-direction. The adsorption energy (E_{ads}) of the CO₂ over model Co₁-Cu₁₂/ZnO (100) surfaces were calculated following the equation:

$$E_{\text{ads}} = E_{\text{surface+CO}_2} - (E_{\text{surface}} + E_{\text{CO}_2, \text{ gas}}) \quad (1)$$

where $E_{\text{surface+CO}_2}$, E_{surface} , and $E_{\text{CO}_2, \text{ gas}}$ denotes the energy of CO₂ adsorbed on the model Co₁-Cu₁₂/ZnO(100) surfaces; the energy of the bare model Co₁-Cu₁₂/ZnO(100) surfaces and energy of CO₂ molecule in the gas phase, respectively.

2. Characterizations for spent catalyst:

Figure S2 shows the XPS spectra for Cu 2p, Zn 2p, Co 2p and Rb 3d in 5Rb5Co-CuZn catalysts, which represents no significant changes after reaction in the oxidation state of the metal present in the catalyst system. Figure S3 and S4 represents the TEM images along with the EDS mapping of spent 5Rb5Co-CuZn shows no agglomeration of particles after reaction. This implies the stability of the catalysts after the reaction.

3. Stability test of the catalyst

To investigate the catalyst's long-term stability, a 48-hour reaction was conducted for the hydrogenation of CO₂ to methanol using the best-performing (5Rb5Co-Cu-ZN) catalyst under optimised conditions. During this period, the catalyst achieved a 23.7% conversion of CO₂ to methanol with a selectivity of 88.2%. Subsequently, the catalysts underwent a recovery process, involving thorough washing and drying, followed by a systematic characterization, including XRD analysis, N₂ physisorption isotherm, and TEM analysis.

In the XRD diffractogram, it was evident that the metallic Cu phase remained unchanged, consistent with JCPDS card no. 03-1019, as depicted in Fig. S5(a). The presence of peaks at $2\theta = 31.7^\circ, 34.4^\circ, 36.3^\circ, 47.5^\circ, 56.6^\circ,$ and 62.8° indicated the existence of ZnO species (JCPDS card no. 36-1451). The N₂ physisorption isotherm exhibited an H4 hysteresis and revealed a BET surface area of 244 m²/g, along with an average pore diameter of 4.34 nm (Fig. S5(b)), which closely resembled the characteristics of the fresh catalyst. TEM micrograph reveals that the particles are well dispersion on the CN_x support, as illustrated in Fig. S5 (c-e). The Cu particle size distribution indicated an average particle size of 9.2 nm, suggesting that no particle agglomeration occurred during the reaction. Additionally, the selected area electron diffractogram (SAED) image confirmed the preserved crystallinity of the catalyst, as shown in Fig. S5(f). These key evidences gathered from the characterisation of the spent catalyst demonstrates that the catalyst maintains remarkable stability over an extended duration in an aqueous phase.

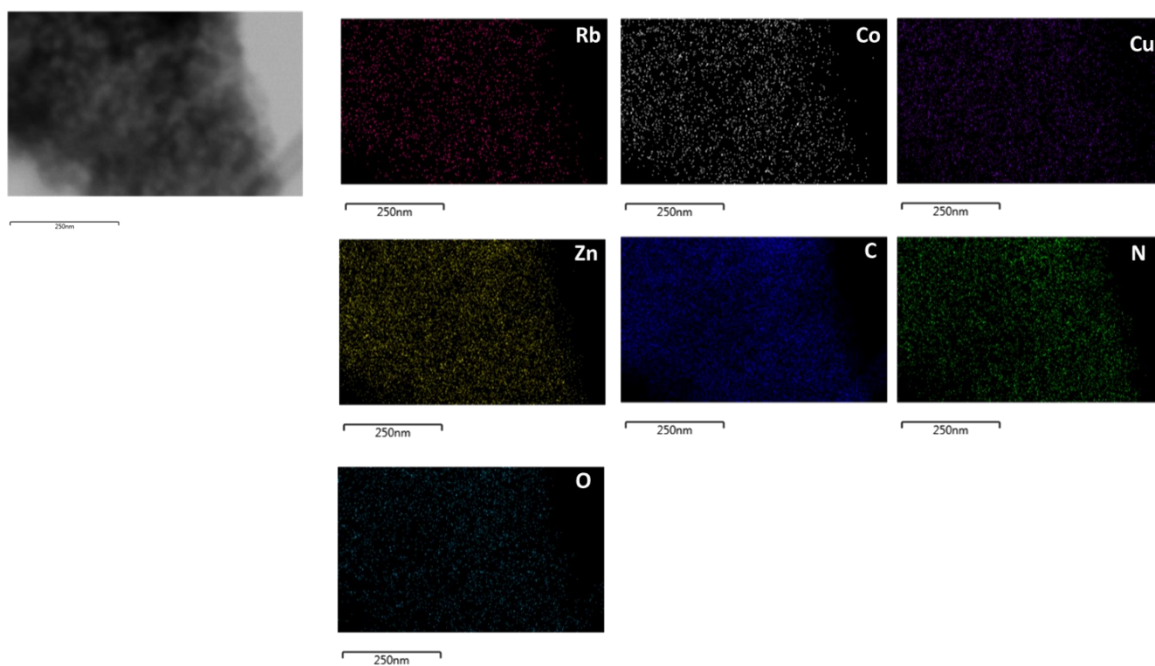


Figure S1: EDS mapping for fresh 2.5Rb5Co-CuZn catalyst

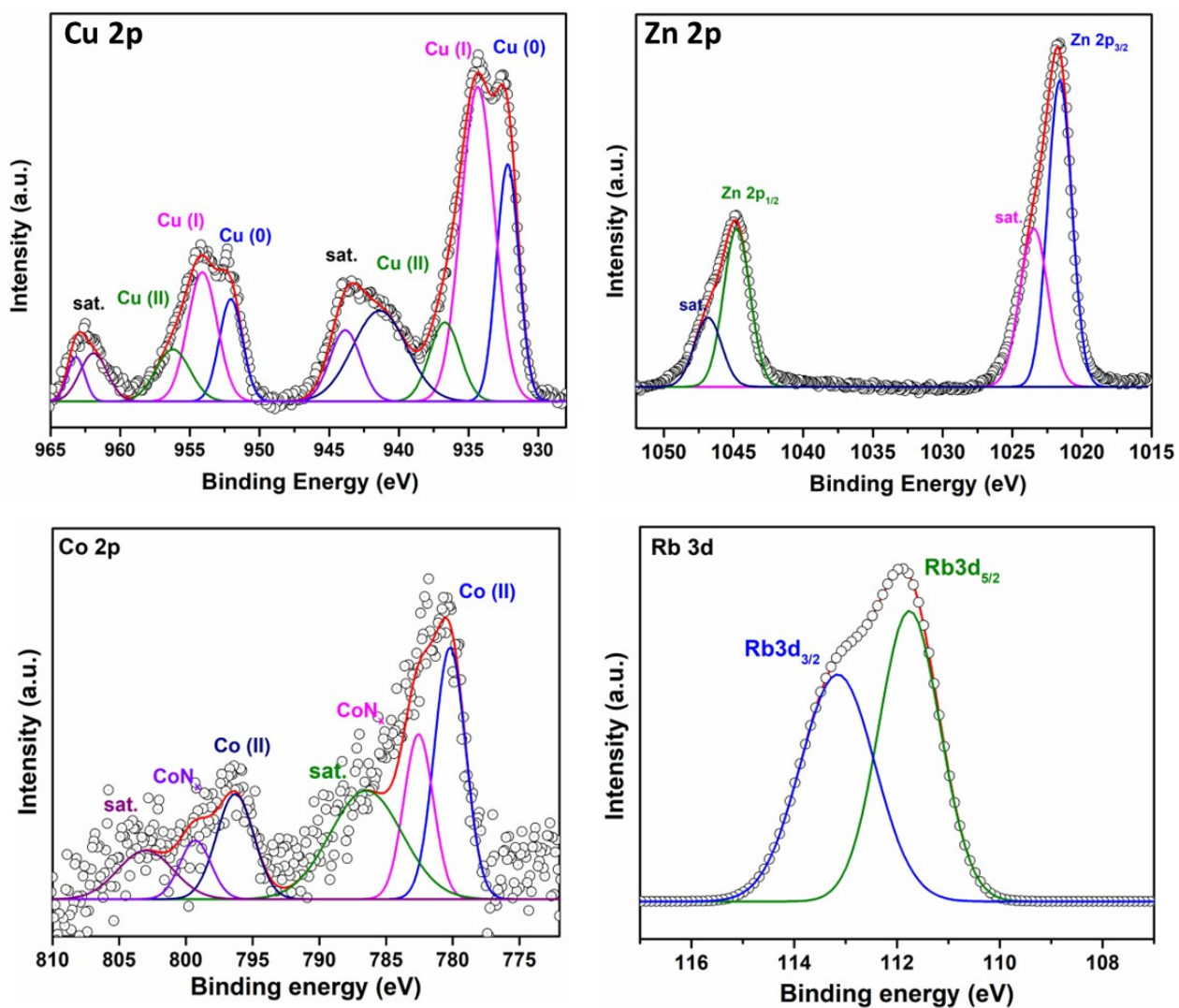


Figure S2: XPS spectra for spent 5Rb5Co-CuZn

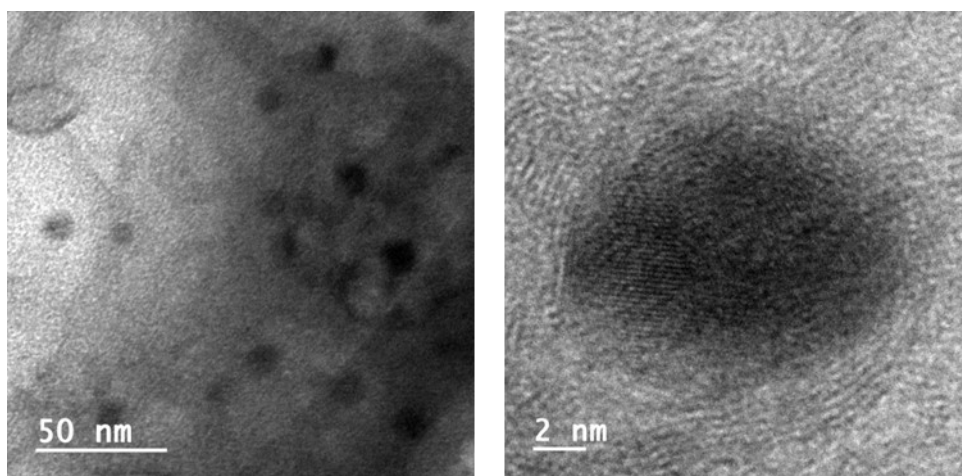


Figure S3: TEM images for spent 5Rb5Co-CuZn

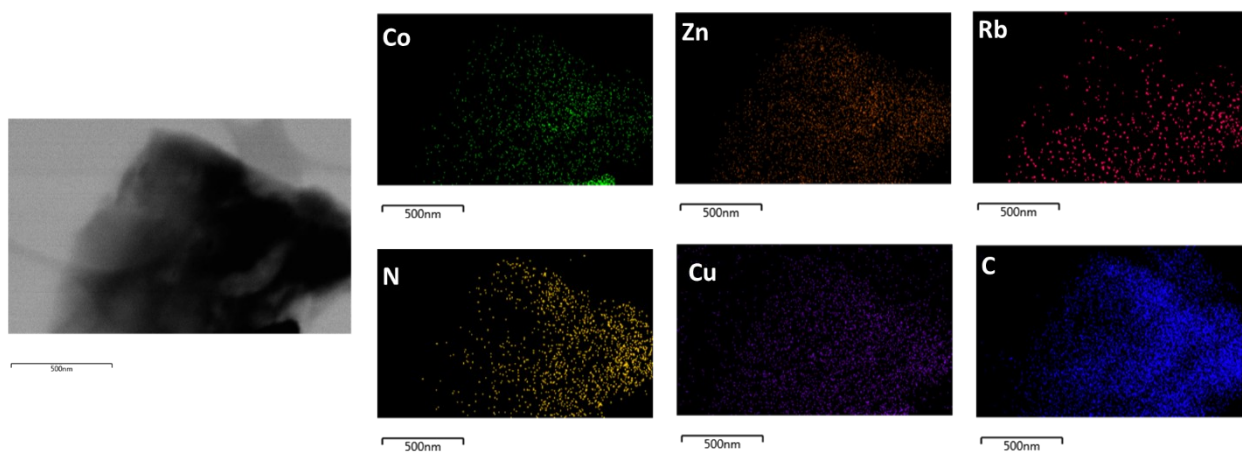


Figure S4: Elemental mapping of spent 5Rb5Co-CuZn

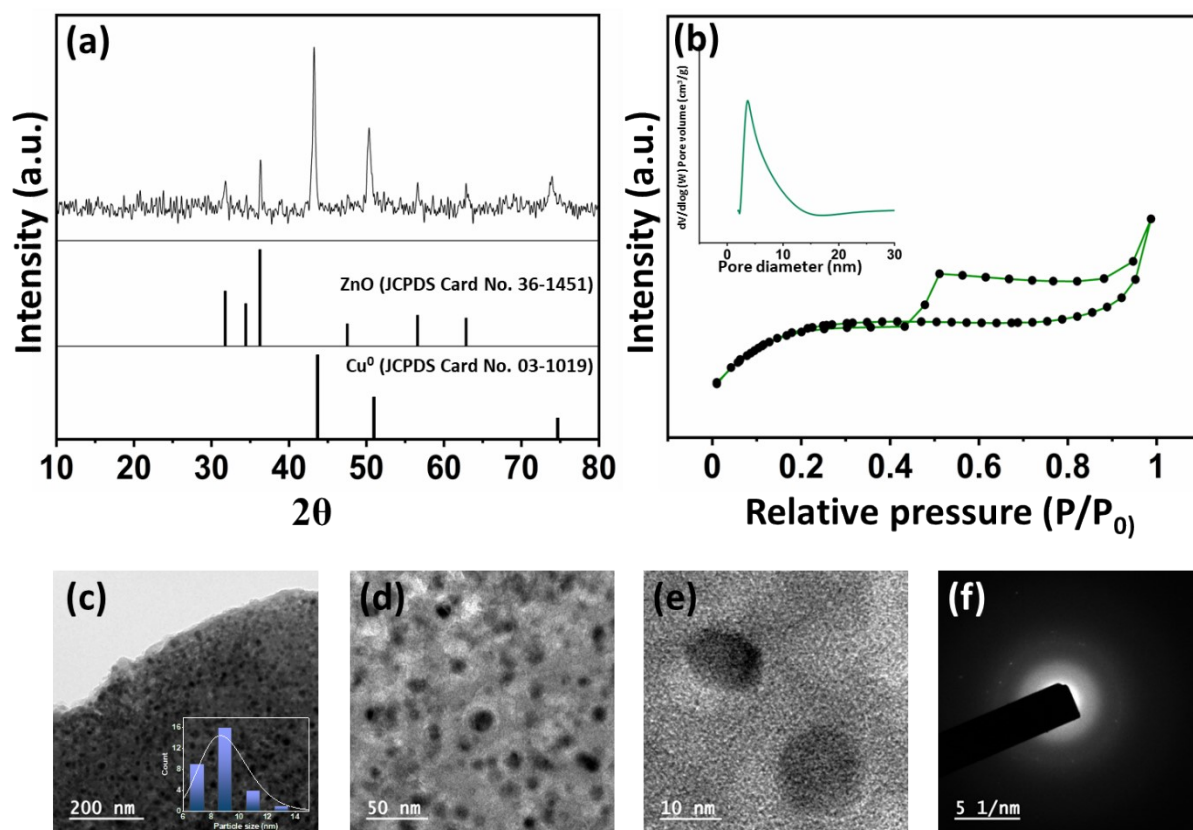


Figure S5: Characterization of spent 5Rb5Co-CuZn catalyst (a) XRD (b) N₂ physisorption isotherm, (inset) pore size distribution (c) TEM images, (inset) particle size distribution (e) HR-TEM (f) SAED

Table S1: Surface area, surface composition determined from EDS mapping, and total CO₂ uptake

Catalyst	Surface Composition (at. %)			Surface area (m ² /g)	Total CO ₂ uptake (mmol/g)
	Cu	Zn	Co		
2.5Na5Co-CuZn	1.78	3.2	0.5	235	0.99
2.5K5Co-CuZn	1.85	3.1	0.6	230	1.38
2.5Rb5Co-CuZn	1.79	3.5	0.6	251	2.52
2.5Cs5Co-CuZn	1.70	3.4	0.5	288	3.82

Table S2: AFTS activity and selectivity for different dispersible NPs and supported catalyst

Sl. No.	Catalyst	Loading	P (MPa) (CO ₂ +H ₂ =3:1)	T (K)	Product Yields /mmolg ⁻¹ h ⁻¹	Selectivity (%)	CO ₂ conversion	Ref
1	Cu-UiO-66	1	1	448	-	100	1	5
2	Cu-UiO-66	1.4	3.2	523	679.76	29.6	-	6
3	Cu@3D-ZrOx	12.4	4.5	533	796	78.8	13.1	7
4	Cu/ZnOx@UiO-66	5.9	4	523	28.3	87	4.3	8
5	Cu/ZnOx@UiO-bpy	6.9	4	523	37.5	100	3.3	9
6	Cu-ZrO ₂ (ZrO ₂ @HKUST-1)	11	3	493	287.9	64.4	6.8	10
7	ZnO/Cu(Cu@ZIF-8)	57.6	4.5	533	933	-	-	11
8	PdZn (Cu@ZIF-8)	-	4.5	543	650	55	14	12
9	In ₂ O ₃ /Co ₃ O ₄ (In@ZIF-67)	-	5	573	650	87	-	13
10	5Rb5Co-CuZn	-	6	473	-	89	24	This work

Table S3: The representation of deviation in CO₂ hydrogenation for 5Rb5Co-CuZn catalyst

Batch	Conversion (%)	Selectivity (%)			
		Methanol	Ethanol	CH₄	CO
Batch 1	24.0	89.2	5.3	2.3	3.2
Batch 2	24.1	90.4	5.1	2.7	1.8
Batch 3	22.8	89.1	5.7	2.3	2.9
Batch 4	23.7	87.6	5.4	2.5	4.5
Average	23.7	89.1	5.4	2.5	3.1
Standard deviation	0.6	1.1	0.3	0.2	1.1

3. References:

- 1 D. M. Schubert, D. T. Natan and C. B. Knobler, *Inorganica Chim Acta*, 2009, 362, 4832–4836.
- 2 G. Kresse and J. Furthmüller, *Comput Mater Sci*, 1996, 6, 15–50.
- 3 J. M. Smith, S. P. Jones and L. D. White, *Gastroenterology*, 1977, 72, 193.
- 4 B. Hammer, L. B. Hansen and J. K. Nørskov, *Phys Rev B Condens Matter Mater Phys*, 1999, 59, 7413–7421.
- 5 B. Rungtaweevoranit, J. Baek, J. R. Araujo, B. S. Archanjo, K. M. Choi, O. M. Yaghi and G. A. Somorjai, *Nano Letters*, 2016, 16, 7645–7649.
- 6 Y. Zhu, J. Zheng, J. Ye, Y. Cui, K. Koh, L. Kovarik, D. M. Camaioni, J. L. Fulton, D. G. Truhlar, M. Neurock, C. J. Cramer, O. Y. Gutiérrez and J. A. Lercher, *Nature Communications*, DOI:10.1038/s41467-020-19438-w.
- 7 T. Liu, X. Hong and G. Liu, *ACS Catalysis*, 2020, 10, 93–102.
- 8 Y. Yang, Y. Xu, H. Ding, D. Yang, E. Cheng, Y. Hao, H. Wang, Y. Hong, Y. Su, Y. Wang, L. Peng and J. Li, *Catalysis Science and Technology*, 2021, 11, 4367–4375.
- 9 B. An, J. Zhang, K. Cheng, P. Ji, C. Wang and W. Lin, *Journal of the American Chemical Society*, 2017, 139, 3834–3840.
- 10 J. Yu, S. Liu, X. Mu, G. Yang, X. Luo, E. Lester and T. Wu, *Chemical Engineering Journal*, 2021, 419, 129656.
- 11 B. Hu, Y. Yin, Z. Zhong, D. Wu, G. Liu and X. Hong, *Catalysis Science and Technology*, 2019, 9, 2673–2681.
- 12 Y. Yin, B. Hu, X. Li, X. Zhou, X. Hong and G. Liu, *Applied Catalysis B: Environmental*, 2018, 234, 143–152.
- 13 A. Pustovarenko, A. Dikhtiarenko, A. Bavykina, L. Gevers, A. Ramírez, A. Russkikh, S. Telalovic, A. Aguilar, J. L. Hazemann, S. Ould-Chikh and J. Gascon, *ACS Catalysis*, 2020, 10, 5064–5076.